Cell Research (2016) 26:556-573.

www.nature.com/cr

ORIGINAL ARTICLE

Positive selection rather than relaxation of functional constraint drives the evolution of vision during chicken domestication

Ming-Shan Wang[1, 3], Rong-wei Zhang[7], Ling-Yan Su[2, 3], Yan Li[1, 3], Min-Sheng Peng[1, 3], He-Qun Liu[1, 3], Lin Zeng[1, 3], David M Irwin[1, 5, 6], Jiu-Lin Du[7], Yong-Gang Yao[2, 3], Dong-Dong Wu[1, 2], Ya-Ping Zhang[1, 3, 4]

[1]State Key Laboratory of Genetic Resources and Evolution, Yunnan Laboratory of Molecular Biology of Domestic Animals, [2]Key Laboratory of Animal Models and Human Disease Mechanisms of the Chinese Academy of Sciences & Yunnan Province, Kunming Institute of Zoology, Kunming, Yunnan 650223, China; [3]Kunming College of Life Science, Unisversity of Chinese Academy of Sciences, Kunming, Yunnan 650204, China; [4]Laboratory for Conservation and Utilization of Bio-resource, Yunnan University, Kunming, Yunnan 650091, China; [5]Department of Laboratory Medicine and Pathobiology, University of Toronto, Toronto, Canada; [6]Banting and Best Diabetes Centre, University of Toronto, Toronto, Canada; [7]Institute of Neuroscience and State Key Laboratory of Neuroscience, Shanghai Institutes for Biological Sciences, Chinese Academy of Sciences, Shanghai 200031, China

As noted by Darwin, chickens have the greatest phenotypic diversity of all birds, but an interesting evolutionary difference between domestic chickens and their wild ancestor, the Red Junglefowl, is their comparatively weaker vision. Existing theories suggest that diminished visual prowess among domestic chickens reflect changes driven by the relaxation of functional constraints on vision, but the evidence identifying the underlying genetic mechanisms responsible for this change has not been definitively characterized. Here, a genome-wide analysis of the domestic chicken and Red Junglefowl genomes showed significant enrichment for positively selected genes involved in the development of vision. There were significant differences between domestic chickens and their wild ancestors regarding the level of mRNA expression for these genes in the retina. Numerous additional genes involved in the development of vision also showed significant differences in mRNA expression between domestic chickens and their wild ancestors, particularly for genes associated with phototransduction and photoreceptor development, such as *RHO* (rhodopsin), *GUCA1A*, *PDE6B* and *NR2E3*. Finally, we characterized the potential role of the *VIT* gene in vision, which experienced positive selection and downregulated expression in the retina of the village chicken. Overall, our results suggest that positive selection, rather than relaxation of purifying selection, contributed to the evolution of vision in domestic chickens. The progenitors of domestic chickens harboring weaker vision may have showed a reduced fear response and vigilance, making them easier to be unconsciously selected and/or domesticated.

***Keywords*:** chicken domestication; unconscious selection; genome evolution; evolution of vision
Cell Research (2016) **26**:556-573. doi:10.1038/cr.2016.44; published online 1 April 2016

Introduction

As noted by Darwin, chickens have the greatest phenotypic diversity among birds. Compared with their wild ancestor, the Red Junglefowl, domestic chickens harbor many typical domestication characteristics, such as larger body size, tame behavior, and higher egg productivity. Identifying the genetic changes underlying these phenotypic changes should provide new insights into the successful domestication of animals and further inform future breeding programs. A pioneering study by Rubin *et al*. [1] used re-sequencing of genomes of commercial chickens as well as populations of Red Junglefowl to identify several selective sweeps associated with reproduction and growth. However, their approach had

Correspondence: Dong-Dong Wu[a], Ya-Ping Zhang[b]
[a]E-mail: wudongdong@mail.kiz.ac.cn
[b]E-mail: zhangyp@mail.kiz.ac.cn
Received 26 August 2015; revised 18 January 2016; accepted 22 February 2016; published online 1 April 2016

limitations in comprehensively elucidating the genetic differences that account for the phenotypic differences between domestic chickens and Red Junglefowl. This was due to, for example, the use of commercial chickens that evolved from Red Junglefowl under strong selection by humans for specific traits associated with growth (e.g., meat production) and reproduction (e.g., egg production) as wells as the use of pooled re-sequenced genomes. Despite the great leap in genetic technologies witnessed in the recent past, the genetic mechanisms underlying many interesting evolutionary differences between domestic chickens and their wild ancestors, for example, reduced vision prowess in chickens, remain unclear.

Vision is one of the most crucial abilities affecting the survival of animal species, as it influences an array of core behavioral traits associated with mating, foraging, and predator avoidance [2]. However, domesticated animals including dogs, horses, and chickens, which are bred and protected by humans, seem to exhibit markedly weaker visual acuity compared to their wild counterparts [3-7]. Domestic chickens (except game fowl) share with these other domestic animals a reduced visual ability as compared to the Red Junglefowl, assumedly the cost of domestication due to the relaxation of selective constraints. The living condition changes that accompany domestication are a reflection of human interventions such as offering protection, provision of food and promotion of the animal breeding. These interventions reduce the pressure for sharp vision in the domestic chickens [3, 4]. However, unlike other phenotypic differences like growth and reproduction [1], no reports exist for the genetic mechanisms behind the change in visual acuity observed in domestic chickens.

To promote a better understanding of the underlying genes/variants responsible for phenotypic changes that occurred in the domestic chickens, specifically reduced visual capability, we generated genome sequences with high coverage (average ~18.9×) from Red Junglefowl and indigenous chickens bred in villages of Yunnan province, Southwest China, one of the regions where domestic chickens originated from [8]. Based on these genomes, we characterized potential mechanisms underlying the phenotypic evolution of domestic chickens by comparing genome sequences and integrating transcriptome data from different sub-regions of the brain and the retina.

Results

Positively selected genes in domestic chickens compared with the Red Junglefowl

Variants/genes underlying phenotypic changes in the domestic chicken likely evolved rapidly after domestication. Based on the genomic variation data obtained in this study, we identified candidate genes that potentially underwent rapid evolution in the domestic chickens, and thus might have contributed to the phenotypic differences between domestic chickens and the Red Junglefowl. We first employed an outlier approach to identify candidate selected genes based on the empirical data. This method is free from assumptions of demographic history and is considered to be robust to the confounding effect of population demographic history. Typically, regions or loci evolving rapidly that have experienced selection would show specific signatures of variation, including high population differentiation, significantly reduced nucleotide diversity levels and long-range haplotype homozygosity [9]. Based on these principles, we examined four different parameters to identify footprints of artificial selection associated with the evolution and domestication of chicken (Figure 1, Supplementary information, Figure S1): F_{ST} [10], nucleotide diversity (*Pi*), cross-population extended haplotype homozygosity (XP-EHH) [11] and the cross-population composite likelihood ratio (XP-CLR) [12]. The first percentile rank was used as a threshold to identify candidates throughout the analysis.

A number of protein-coding genes with significant higher F_{ST} (184 genes), XP-EHH (212 genes), XP-CLR (335 genes), and a lower value for nucleotide diversity (*Pi* , 284 genes) were identified, and considered to be potential candidate genes that experienced selection during domestication. Of these genes, only 36 were identified by all four methods (Figure 1C, Supplementary information, Table S12). It is not surprising that the overlap among the positively selected genes (PSGs) detected by the different statistical approaches was underwhelming. First, the distinct statistics applied to scan the genome for positive selection are based on different signatures of population variation [9]. Another reason might be attributable to a pitfall in the outlier approach, whereby an outlier value in one analysis, falling in the 99th percentile of the empirical distribution, may not be classified as an outlier in another study where it may fall within the 98th percentile of the study's empirical distribution [13]. This pattern is very common in studies on positive natural selection in humans. For example, only ~14.1% loci were identified in two or more studies with large-scale genome-wide scans of PSGs [13]. In the current study, possibly due to the above stated factors, no significant enrichment for any functional category associated with vision was found among the candidates identified by the F_{ST} test.

Gene ontology (GO) analysis for the genes showing signatures of positive selection pointed out a significant enrichment for categories associated with the develop-

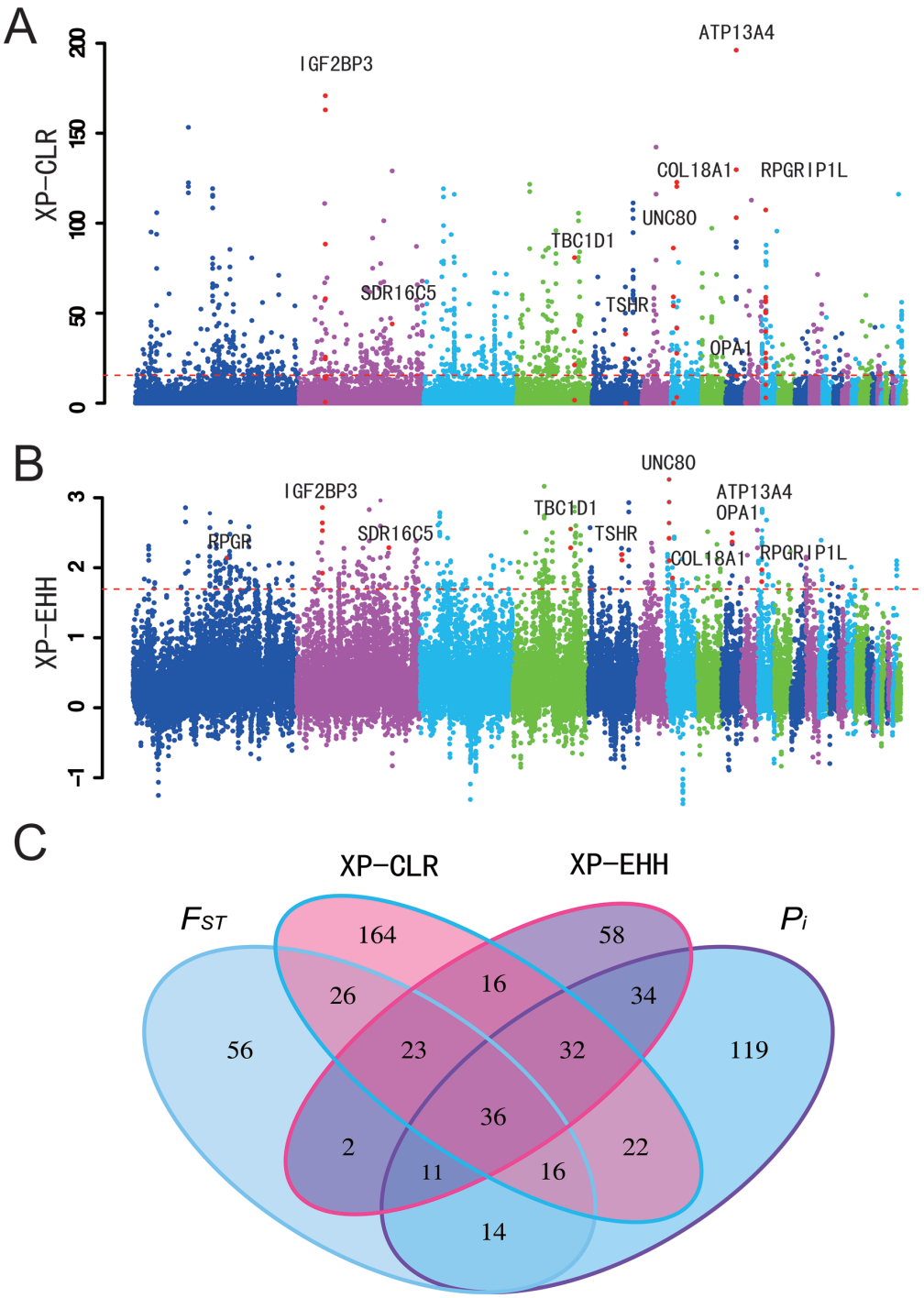

Figure 1 Analysis of the signatures of positive selection in the genome of domestic chickens. Genomic landscape of the XP-CLR values **(A)** and XP-EHH values **(B)** in the genome of domestic chickens. **(C)** Numbers of PSGs identified by the four methods listed in each of the Venn diagram components.

ment of the nervous system (Supplementary information, Tables S8-S11). This finding is not a surprise and is consistent with the rapid evolution of genes in the nervous systems of other domestic animals, which has collectively been attributable to behavioral shifts that accompany domestication [14-18]. In addition, functional enrichment analysis of genes in regions with the top 1% XP-EHH scores revealed that many candidate genes related to the

nervous system were over-represented in the following Human Phenotype Ontology (HPO) categories: abnormality of the nervous system (31 genes), abnormality of the central nervous system (30 genes), and cognitive impairment (25 genes) ($P < 0.05$) (Supplementary information, Table S8). After retrieving regions with the top 1% F_{ST} values, we found that 15 genes significantly over-represented in the HPO categories are related to brain disorders — abnormality of the hindbrain, abnormality of the metencephalon, and abnormality of the cerebellum (Supplementary information, Table S9). Our analysis also picked out these functional categories as regions with low nucleotide diversity (Supplementary information, Table S10). Taken together, these findings suggest that genes involved in both the function and development of the central nervous system showed strong directional selection, which may underlie some of the behavioral alterations occurring during chicken domestication.

For the top 10 SNPs with the highest XP-EHH values, only a single protein-coding gene, *ATP13A4*, was identified. The XP-CLR test also showed that this gene had the most significant XP-CLR values at 10-kb, 5-kb and 2-kb grid sizes (Figure 1; Supplementary information, Figure S2). *ATP13A4* plays vital roles in early neuronal development [19]. It is highly expressed in specific areas of the brain, including the lateral inferior frontal cortex and the temporoparietal cortex, and is associated with benign epilepsy with centrotemporal spikes [20]. It is also associated with speech apraxia among human children [21, 22]. These results collectively suggest that *ATP13A4* likely plays a key role in behavioral evolution during chicken domestication. Similarly, the gene *UNC80*, which has a function in the nervous system [23, 24], also experienced positive selection and had the highest identified XP-EHH score by the sliding window analysis (Figure 1B).

We also identified several other PSGs that are involved in body size development and growth rate, indicative of their role in evolution of the comparatively larger body size among domestic chickens compared to the Red Junglefowl. For example, using different analyses, we identified two genes, *TSHR* and *TBC1D1*, both of which were previously reported to regulate seasonal reproduction and growth among domestic chickens [1, 25]. *IGF2BP3* was identified by its high score in the 10-kb grid size XP-CLR test (Figure 1), and further supported by the 5-kb and 2-kb grid size analyses (Supplementary information, Figure S2). Three other methods that we used in the present study further detected selection signals for this gene (Figure 1, Supplementary information, Figure S1). This is not entirely surprising, as *IGF2BP3*, an important member of the insulin-like growth factor binding protein family, has pro-growth functions via regulating *IGFs* (*IGF1* and *IGF2*) to modulate the insulin signaling pathway [26-28]. Moreover, *IGF2BP3* is located within a QTL region associated with chicken body size (http://www.animalgenome.org/cgi-bin/QTLdb/GG/index) and has differential expression in the muscles of dwarf and normal-sized chickens [29].

To further confirm the findings in this study, we used the Sanger sequencing method to re-sequence and genotype 67 SNPs that cover seven candidate PSGs, *TSHR*, *ATP13A4*, *RPGRIP1L*, *COL18A1*, *VIT*, *OPA1* and *IGF2BP3*, in larger chicken populations. We found that the SNPs genotyped in the larger populations still showed higher F_{ST} values, which is strongly correlated with the genomic analysis ($P < 0.00001$) (Supplementary information, Figure S3 and Table S5). When we compared our candidate PSGs with those identified in the study of Rubin *et al*. [1], only a limited number of genes were shared (Supplementary information, Figure S9). Two important genes, *TSHR* and *TBC1D1*, previously reported by Rubin *et al*. to be involved in regulation of seasonal reproduction and growth in domestic chickens, were again identified to undergo positive selection in our study by the four methods applied.

Positive selection rather than relaxation of purifying selection of vision-related genes in domestic chickens

An additional group of genes possessing signatures of positive selection among the tested domestic chickens was found to be significantly enriched for categories associated with the development and maintenance of the eye as well as vision. Particularly, the PSGs detected by the XP-CLR and *Pi* tests included abnormality of the posterior segment of the eye (19 genes, HP:0004329), nystagmus (18 genes, HP:0000639), abnormality of the fundus (18 genes, HP:0001098), aplasia/hypoplasia affecting the eye (10 genes, HP:0008056), and visual loss (5 genes, HP:0000572) (full details in Table 1). Specific examples in this group are *ZNF469* and *RD3*, with selection signals supported by both XP-CLR and *Pi*, which have vital roles in vision. *ZNF469* encodes a zinc-finger protein and mutations in this gene are associated with brittle cornea syndrome and keratoconus, a common inherited ocular disorder resulting in progressive corneal thinning [30, 31]. *RD3* on the other hand encodes retinal degeneration 3 protein, and mutations in this gene cause Leber congenital amaurosis type 12, a disease that results in photoreceptor degeneration [32].

Positive selection on vision-related genes in the domestic chicken was unexpected since domestic chickens, as previously reported, have a significantly weakened vision compared to their ancestor, the Red Junglefowl [3-5]. Several other studies have proposed that the weakened

Table 1 Gene functional enrichment categories involved in the vision function found in positively selected genes detected by the methods *Pi*, XP-CLR and XP-EHH, and differentially expressed genes detected by Cuffdiff in retina

Methods	*P*-value*	Gene number	Term	Type	Description
Pi	0.0268	5	HP:0000572	hp	Visual loss
(top 1%)	0.0084	4	HP:0000519	hp	Congenital cataract
	0.0184	19	HP:0004329	hp	Abnormality of the posterior segment of the eye
	0.0394	18	HP:0001098	hp	Abnormality of the fundus
	0.0175	5	HP:0001103	hp	Abnormality of the macula
	0.0408	2	HP:0008059	hp	Aplasia/hypoplasia of the macula
XP-CLR	0.0263	4	HP:0000591	hp	Abnormality of the sclera
(top 1%)	0.0163	4	HP:0000592	hp	Blue sclerae
	0.0109	18	HP:0000639	hp	Nystagmus
	0.0118	10	HP:0008056	hp	Aplasia/hypoplasia affecting the eye
	0.0271	5	HP:0008062	hp	Aplasia/hypoplasia affecting the anterior segment of the eye
	0.046	4	HP:0008055	hp	Aplasia/hypoplasia affecting the uvea
	0.0428	4	HP:0008053	hp	Aplasia/hypoplasia of the iris
	0.0204	5	HP:0001103	hp	Abnormality of the macula
	0.0155	2	HP:0000493	hp	Abnormality of the fovea
	0.00277	3	HP:0008061	hp	Aplasia/hypoplasia affecting the retina
	0.00197	3	HP:0008059	hp	Aplasia/hypoplasia of the macula
	0.0105	2	HP:0008060	hp	Aplasia/hypoplasia of the fovea
	0.0105	2	HP:0007750	hp	Hypoplasia of the fovea
XP-EHH	0.0429	3	HP:0000608	hp	Macular degeneration
(top 1%)					
Cuffdiff analyses	0.0262	2	HP:0007663	hp	Decreased central vision
in retina	0.0395	4	HP:0000662	hp	Night blindness
	0.0164	2	HP:0007642	hp	Congenital stationary night blindness
	0.05	4	HP:0000512	hp	Abnormal electroretinogram
	0.05	2	KEGG:04744	ke	Phototransduction

**P*-values are corrected by Benjamini-Hochberg FDR.
No category involved in the vision function was found to be enriched among positively selected genes detected by the F_{ST} method.

visual ability observed in domestic chickens is attributed to relaxation of functional constraints during domestication [3, 4].

Functional enrichment analysis of the 36 genes that overlapped among the candidate gene lists identified by the four different methods showed that several genes are associated with vision-related functional categories — abnormality of the eye/vision (*OPA1*, *COL18A1*, *RPGRIP1L* and *NBAS*), and visual impairment (*OPA1*, *COL18A1* and *RPGRIP1L*) (Supplementary information, Table S13). *COL18A1* encodes the alpha subunit of type XVIII collagen and mutations in this gene are associated with Knobloch syndrome [33, 34], which features high myopia, vitreoretinal degeneration with retinal detachment, and macular abnormalities in humans. *Col18a1*$^{-/-}$ knockout mice display abnormalities in their iris and ciliary bodies, and retina vessel regression. These mice also show abnormal deposits between the basal infoldings of the retinal pigment epithelium, which could result in deterioration of retinal pigment epithelium function and attenuation of visual function as well as pathological electroretinograms (ERG) [35-38]. *OPA1*, encoding a dynamin-like mitochondrial GTPase, is reported to be involved in an autosomal dominant optic atrophy, which is known as Kjer's optic atrophy. It affects retinal ganglion cells and axons forming the optic nerve and leads to progressive visual loss [39, 40].

Demographic history, relaxation of purifying selection and hitchhiking could confound the detection of positive selection. The outlier approach to identify candidate genes used above is based on empirical data that is free from any assumption concerning demographic history, and is considered to be robust to the confounding effects of population demographic history, where genome-wide

forces affect the patterns of variation at all loci in a genome in a similar manner, whereas directional selection specifically acts on certain loci [9]. Notwithstanding the outlier approach already applied, we further performed coalescent simulation analysis based on simulated demographic histories (Supplementary information, Figure S4), and found that the candidate PSGs identified by the outlier approach still harbored statistically significant signals compared with simulated data (Figure 2A-2C). To exclude the possibility that hitchhiking possibly contributed to the signatures of selection on the vision-related genes, we retrieved the vision-related genes potentially

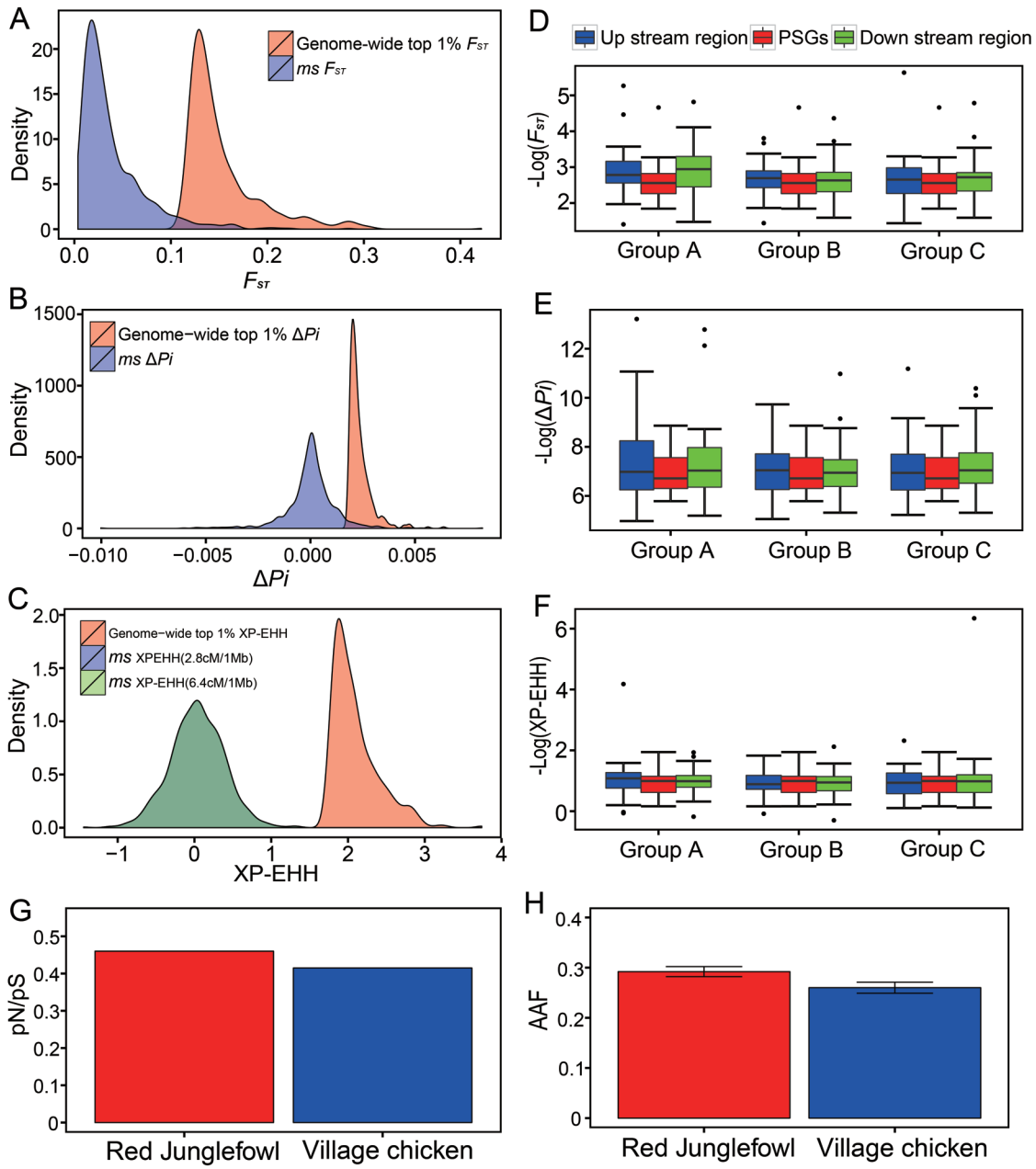

Figure 2 Positive selection on genes involved in vision. **(A-C)** Coalescent simulations (ms) of positive selection detected by F_{ST} **(A)**, *Pi* **(B)** and XP-EHH **(C)**. **(D-F)** F_{ST} **(D)**, *Pi* **(E)** and XP-EHH **(F)** values for the visual-related candidate genes compared with the values for their upstream/downstream sequences with the same length as the gene (Group A), adjacent genes (Group B) and upstream/downstream 50 kb sequences (Group C). **(G)** The ratio of the numbers of non-synonymous SNPs to the numbers of synonymous SNPs (pN/pS). **(H)** the alternative allele frequency (AAF) of the visual-related candidate genes in the village chickens and Red Junglefowl.

undergoing positive selection and compared the pattern of variation in regions upstream and downstream of the genes to that of variation within these vision-related genes. As expected, these vision-related genes harbored higher levels of population differentiation, and higher values of XP-EHH values, than adjacent genes and regions (Figure 2D-2F).

The ratio of non-synonymous to synonymous substitution rates (pN/pS) in the coding sequences was used to assess the relaxation of purifying selection, in which case pN/pS should increase [41, 42]. In this analysis, we retrieved SNPs in vision-related genes identified under potential positive selection by the four methods, and counted the numbers of SNPs unique to the domestic chicken or Red Junglefowl. We found lower pN/pS in domestic chicken than in the Red Junglefowl (Figure 2G). Compared with the Red Junglefowl, domestic chickens harbored a lower frequency of alternative alleles (Figure 2H). In addition, we employed different methods based on different population genetic theories to detect positive selection, which could possibly reduce the false discovery rate due to the relaxation of purifying selection and/or demographic history. Our analyses indicated a strong unlikelihood that relaxation of purifying selection occurred in the genes associated with vision.

Differential expression of PSGs in the retina between domestic chickens and Red Junglefowl

Since our results on positive selection in vision-related genes were somewhat surprising, given previous viewpoints [3, 4], we sought to better understand the evolution of the domestic chicken by sequencing (via RNA-seq) transcriptomes from five tissues (cerebral cortex, corpus striatum, optic lobe, cerebellar vermis, and retina) from the Red Junglefowl and domestic chickens. We calculated differences in expression levels for each gene between Red Junglefowl and domestic chickens (see Materials and Methods). This analysis showed that genes with signatures of positive selection presented significantly higher levels of expressional difference in retinal tissue between the domestic chicken and Red Junglefowl than other genes (Figure 3A-3D, F_{ST}, $P = 0.075$; *Pi*, $P = 2.99 \times 10^{-7}$; XP-CLR, $P = 0.015$; and XP-EHH, $P = 5.50 \times 10^{4}$, Mann-Whitney *U*-test). We sought to verify and replicate this result by profiling another 10 transcriptomes (6 transcriptomes of 3 retina from 3 Red Junglefowls and 4 transcriptomes of 2 retina from 2 village chickens) with two replications per sample using a different sequencing platform (see Materials and Methods). The results remained synonymous to the earlier analysis when the data from two platforms were analyzed separately (Supplementary information, Figure S5A, F_{ST}, $P = 0.104$; *Pi*, $P = 0.018$; XP-CLR, $P = 0.178$; and XP-EHH, $P = 0.005$, Mann-Whitney *U* test), or jointly (Supplementary information, Figure S5B, F_{ST}, $P = 0.040$; *Pi*, $P = 2.23 \times 10^{-4}$; XP-CLR, $P = 0.049$; and XP-EHH, $P = 8.52 \times 10^{-4}$, Mann-Whitney *U* test). However, the four brain regions did not show significantly differential expression patterns except for the corpus striatum by the *Pi* method (Figure 3B, $P = 0.036$, Mann-Whitney *U* test). It is possible that some PSGs are upregulated while others are downregulated in the brains of the village chickens, resulting in the non-significant variations noted when all PSGs were analyzed together. In addition, a greater number of PSGs exhibited expression level changes between the Red Junglefowl and village chicken in the eye than any of the four brain regions (Supplementary information, Figure S6). This pattern supports the hypothesis that positive selection drove changes in the regulation of gene expression that attenuated vision in the domestic chickens.

We then used Cuffdiff [43] to retrieve a series of genes that exhibited significant differential expression between the Red Junglefowl and domestic chicken in the cerebral cortex (137 genes), corpus striatum (24 genes), cerebellar vermis (9 genes), optic lobe (19 genes), and the retina (57 genes). Functional enrichment analysis of the 57 differentially expressed genes in the retina between the Red Junglefowl and domestic chickens showed that four genes (*RPGR*, *GUCA1A*, *TRPM1* and *PDE6B*) were involved in several HPO categories including decreased central vision, congenital stationary night blindness, and abnormal ERG (Table 1). We verified the differential expression of these four genes, as well as two additional genes that are important for vision, *RHO* [44] and *NR2E3* [45-47], via quantitative real-time PCR (qPCR) for retina mRNA (Figure 3E). Differences in gene expression measured by qPCR and RNA-seq were significantly correlated (Figure 3F). The significant changes in the mRNA expression in the retina between Red Junglefowl and the domestic chickens potentially have functional consequences in vision due to their respective functions. For example, *NR2E3* (photoreceptor cell-specific nuclear receptor, group E, member 3) is a vital transcriptional regulator essential for photoreceptor development and differentiation due to its capability as an activator of rod cell development and a repressor of cone development [45-47]. In domestic chickens, downregulation of *NR2E3* expression is associated with weaker visual ability and lower optical sensitivity [3]. Similarly, *RHO* (rhodopsin), *GUCA1A* (guanylate cyclase activator 1A) and *PDE6B* (phosphodiesterase 6B) are all vital genes in the phototransduction pathway [44, 48, 49]. Among domestic chickens, expression of *GUCA1A*, *PDE6B* and *RHO* were downregulated in the retina, suggesting a depres-

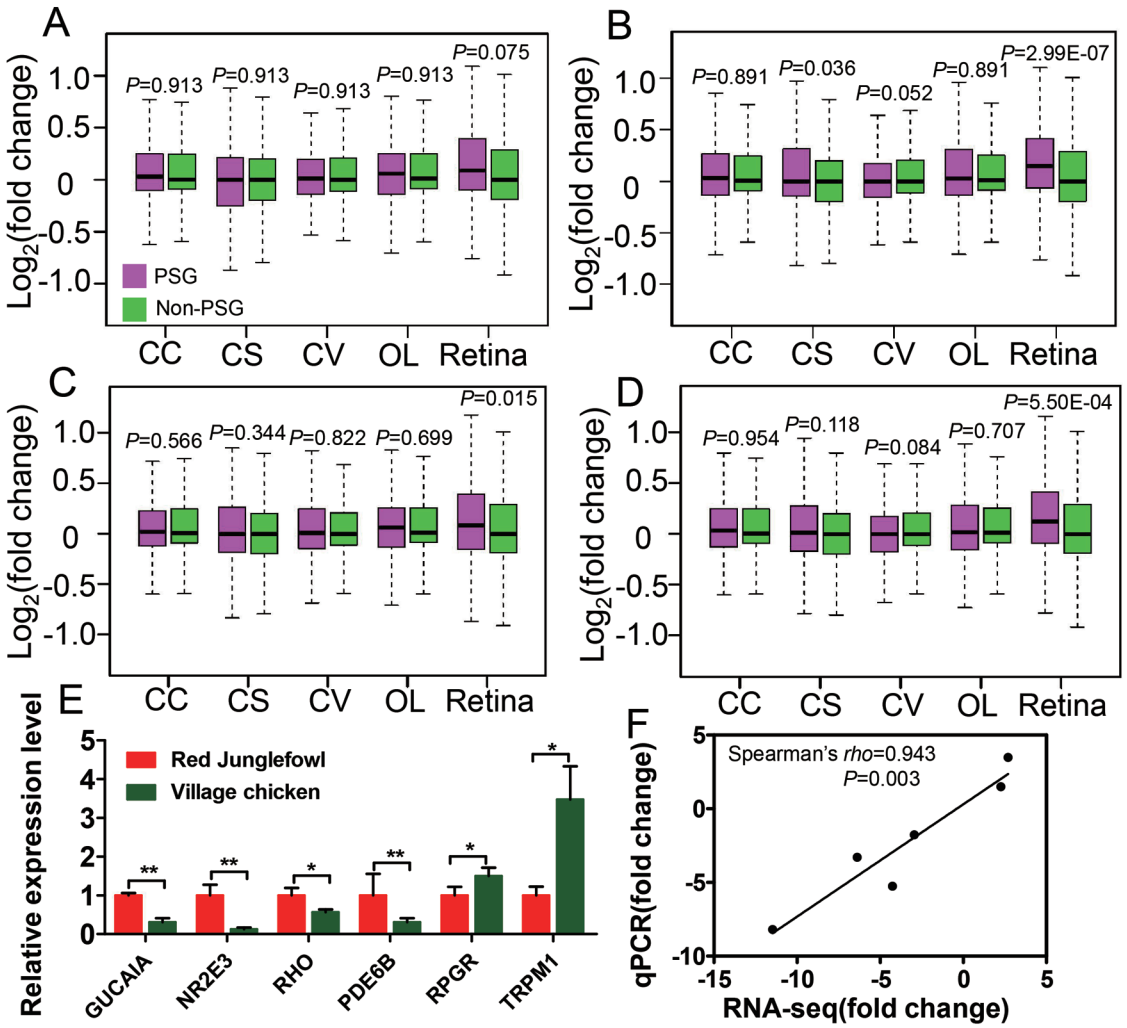

Figure 3 Gene expression for PSGs in five tissues (cerebral cortex (CC), corpus striatum (CS), cerebellar vermis (CV), optic lobe (OL), and retina) comparing domestic chickens and Red Junglefowl. **(A-D)** PSGs as identified by F_{ST} **(A)**, *Pi* **(B)**, XP-CLR **(C)** and XP-EHH **(D)**. **(E)** Difference in expression for six genes between the village chicken and Red Junglefowl in the retina verified by qPCR. **(F)** Correlation of the gene expression measured by qPCR versus RNA-seq. Fold change, implying $(FPKM + 1)_{VC}/(FPKM + 1)_{RJF}$ for each gene. Statistical significance is indicated by *, where $P < 0.05$, and **, where $P < 0.01$.

sion in the phototransduction pathway in the domestic chicken. In addition, *RPRG* and *TRPM1* exhibited upregulation in domestic chickens. Both genes play important roles in vision [50, 51], for instance, *RPGR* encodes a retinitis pigmentosa GTPase regulator and overexpression of a *RPGR* transcript leads to severe photoreceptor degeneration in mice [52].

Functional analysis of VIT, a PSG presumably involved in vision

PSGs presented significantly higher levels of differential gene expression in retinal tissue between the domestic chicken and Red Junglefowl and differentially expressed genes in retinal tissue were also involved in visual ability. However, only two genes, *RPGR* and *VIT*, were identified to undergo positive selection in domestic chicken (Figure 1B; Supplementary information, Figure S1B; Figures 3E, 4A-4C). *RPGR* was supported with signal of positive selection by both *Pi* and XP-EHH tests (the first percentile rank as threshold) (Figure 1B; Supplementary information, Figure S1B) and had an increased level of expression in village chickens compared to Red Junglefowl (Figure 3E). Mutations in *RPGR* are associated with X-linked retinitis pigmentosa (XLRP) and result in severe and progressive loss of vision in dogs and humans [50]. The second gene, *VIT*, showed a higher level of population differentiation (F_{ST}) and lower level of nucleotide diversity (*Pi*) in village chickens (Figure 4A),

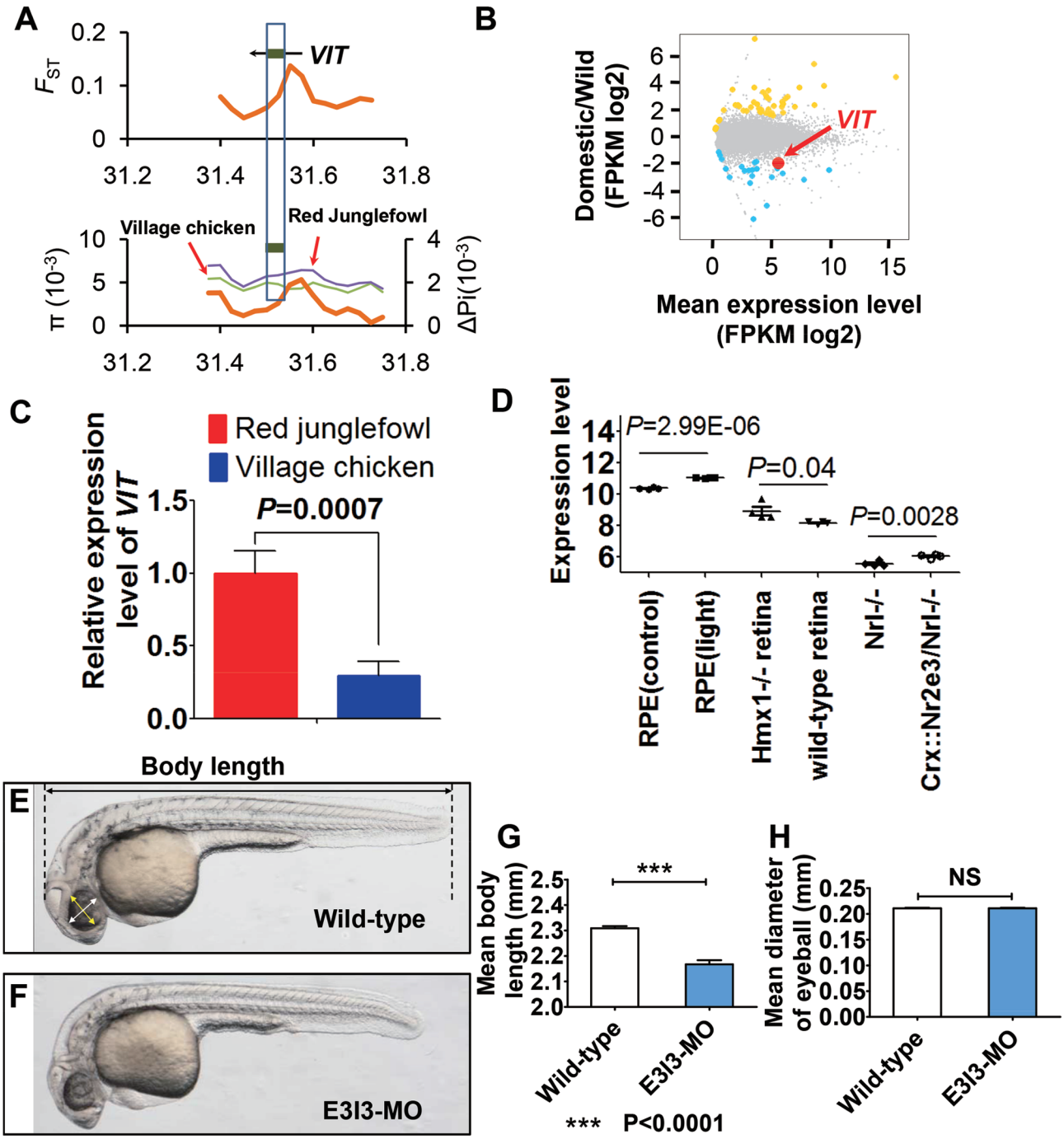

Figure 4 Signal of positive selection and knockdown array of *VIT* in zebrafish. **(A)** F_{ST} and *Pi* values showed selection signal for *VIT* gene. **(B)** RNA-seq analysis presented differential expression of *VIT*. **(C)** qPCR confirmation of the downregulation of *VIT* in retinal tissue between the domestic chicken and Red Junglefowl. **(D)** Expression analysis of *VIT* in mice. Expression profiling in retinal pigment epithelium (RPE) of mice exposed to 10 000 lux of cool white fluorescent light for 18 h was based on expression data of retina from *Hmx1* loss-of-function mice (GSE37773) and wild-type mice (GSE47002), and expression data from photoreceptor cells of *Nrl*$^{-/-}$ mice and *Crx::Nr2e3/Nrl*$^{-/-}$ mice (GSE5338). **(E-F)** Lateral view of a zebrafish with measurements of body length **(E)** and eyeball diameter **(F)**. Scale bar, 0.5 mm. **(G-H)** Body lengths **(G)** and eyeball diameters **(H)** of embryos injected with *VIT-e3i3*-MO (E3I3-MO) or wild-type control at 32 h post-fertilization (hpf) (*VIT* morphants and control embryos, *n* = 10 each; mean ± SEM). Body length is significantly decreased in *VIT* morphants; **P* < 0.0001; NS, not significant.

and was found to show significant differential expression in the retinal tissue in domestic chicken compared to Red Junglefowl (Figure 4B). Results from qPCR further confirmed the downregulation of *VIT* in the village chicken compared with Red Junglefowl (Figure 4C). Until now, the function of *VIT* remains unclear. However, it demonstrated specific expression in the eye in the mice (Supplementary information, Figure S7), leading us to reason that *VIT* is likely involved in vision and that downregulation of *VIT* expression might play a role in the evolution of vision in domestic chicken.

To obtain a better understanding of the function of *VIT,* we first examined the *VIT* expression data available for the mouse. Expression of *VIT* was significantly upregulated in the retinal pigment epithelium of mice after exposure to 10 000 lux of cool white fluorescent light for

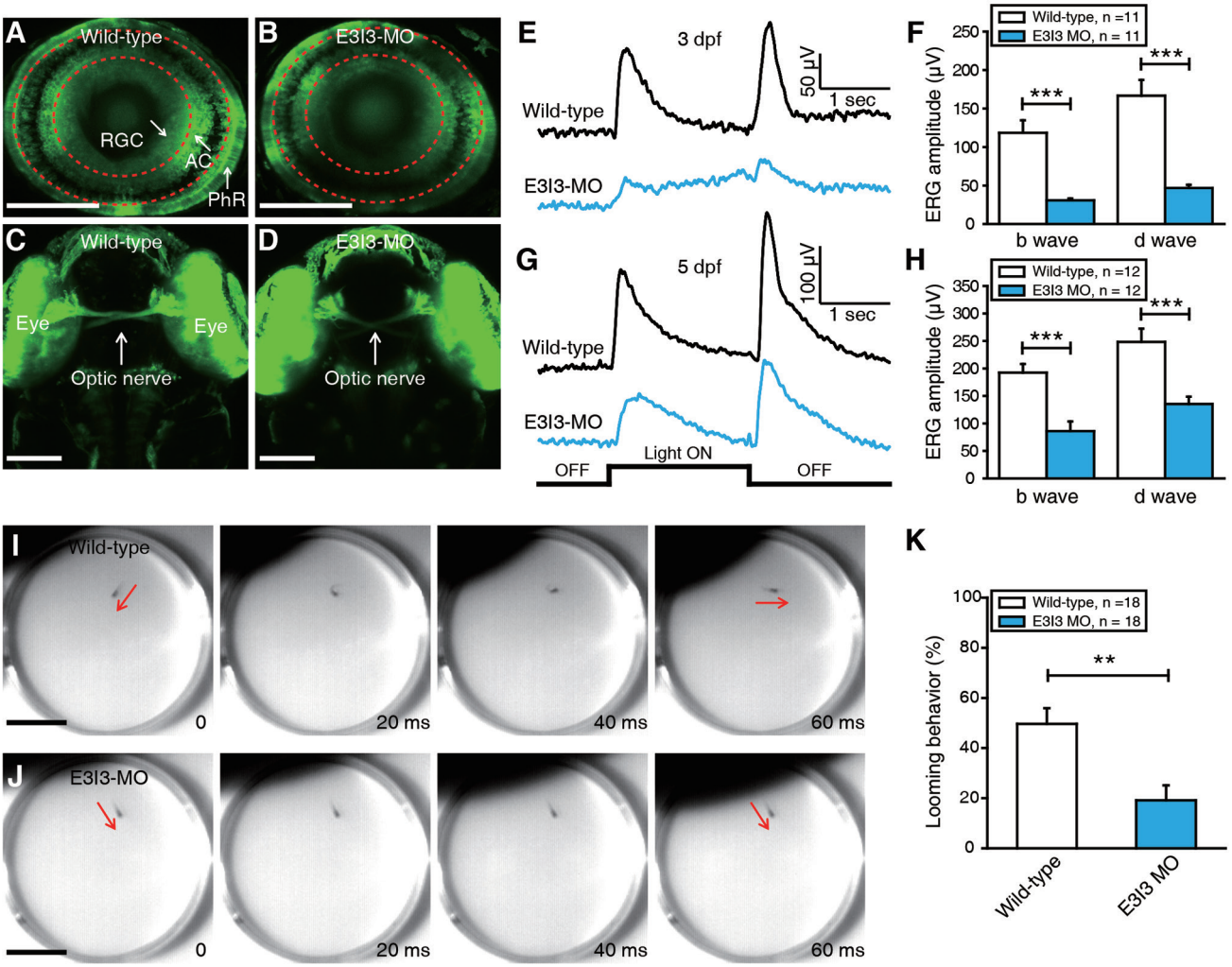

Figure 5 Electrophysiological recordings and behavioral tests showed that *VIT* is necessary for normal physiological function of zebrafish retina. **(A**, **B)** Confocal images showing GCaMP1.6 expression in photoreceptors (PhR), retinal ganglion cells (RGC) and amacrine cells (AC) of a 3-dpf Tg (Ath5-gal4:UAS-GCaMP1.6) larva **(A)** and a *VIT* morphant **(B)**. The two red dash circles indicate the position of inner and outer plexiform layers. Scale bar, 100 μm. **(C**, **D)** Confocal images showing the projection of optic nerves from two eyes of a 3-dpf wild-type larva **(C)** and a *VIT* morphant **(D)**. Scale bar, 100 μm. **(E**, **G)** ERG recording averaged from ten responses to a 2-s light ON stimulus in 3-dpf **(E)** or 5-dpf **(G)** wild-type larvae and *VIT* morphant. **(F**, **H)** Summary of ERG recording data at 3 **(F)** or 5 dpf **(H)**. **(I**, **J)** Examples showing a looming stimulus-induced escape behavior in a 5-dpf wild-type larva **(I)**, but not in a 5-dpf *VIT* morphant **(J)**. The red arrows indicate the body axis of the larvae before and after looming-induced C-startle escape. Scale bar, 1 cm. **(K)** Summary of data showing the probability of looming-induced escape behaviors in 5-dpf wild-type larvae and *VIT* morphant. The number in the inset of **F**, **H** and **K** represents the number of larvae examined. $^{**}P < 0.01$, $^{***}P < 0.001$; two-tailed unpaired Student's *t*-test for the data in **F**, **H** and **K**. Data are represented as mean ± SEM.

18 h (Figure 4D). Expression of *VIT* also changed after the knockout of several genes that are crucial for the development of vision. For example, *VIT* was upregulated in the retina of *Hmx1*-knockout mice (Figure 4D). *Hmx1* (H6 family homeobox 1) is a transcription factor crucial for the development of the eye. Other transcriptional regulators like *NRL*, *CRX* and *NR2E3*, are also important for photoreceptor differentiation [46]. From a past study, endogenous *NR2E3* transcript or protein was not detectable in the retina of $Nrl^{-/-}$ mice [46]. However, when exogenous *NR2E3* was expressed in post-mitotic photoreceptor precursors using the *Crx* promoter in $Nrl^{-/-}$ mice, expression of *VIT* was significantly upregulated (Figure 4D). Consistently, the expression levels of both *NR2E3* and *VIT* were lower in village chicken than in Red Junglefowl. These expression data suggest a potential function of *VIT* in vision.

To further study the function of *VIT*, we performed a knockdown array of *VIT* in zebrafish (*Daniorerio*) embryos by targeting its expression with a specific antisense morpholino (MO) oligonucleotide preventing the proper splicing of exon 3 (E3I3-MO) (Figure 4E-4H). While the body length of *VIT*-knockdown zebrafish is significantly decreased compared with controls (Figure 4G), no significant change in eye size was observed (Figure 4H), suggesting that the phenotypic effects of *VIT* knockdown are in tissues other than the eye in the zebrafish. However, since expression of *VIT* is highly eye-specific in mice (Supplementary information, Figure S7), downregulation of *VIT* might have greater influence on the eye than other tissues in species such as chicken. We then examined the effect of *VIT* knockdown on the general morphology of the zebrafish retina by using Tg (Ath5-gal4:UAS-GCaMP1.6) larvae, where most photoreceptors, retinal ganglion cells and some amacrine cells are labeled with GCaMP1.6 (Figure 5A). Compared with control larvae, the general structure of the retinal layers and the projection of the optic nerves were not changed in the *VIT* morphant (Figure 5A-5D), consistent with the above observation that there is no significant change in eye size between control and *VIT* morphant (Figure 4H).

To determine whether the knockdown of *VIT* gene leads to defective retinal function, we performed electrophysiological recordings and behavioral tests. Application of a 2-s whole-field flash near the eyes of zebrafish elicited a clear ERG response from the eye, where b and d waves occurred at the onset and the offset of the flash, respectively (Figure 5E). Knockdown of *VIT* dramatically decreased the amplitude of b and d waves in both 3-dpf and 5-dpf larvae (Figure 5E-5H). Since b and d waves are generated mainly by ON and OFF bipolar cells, respectively [53], this result indicates that *VIT* might be necessary for the normal function of bipolar cells. Furthermore, we examined the effect of *VIT* knockdown on visual-induced escape behaviors. A looming stimulus, an expanding black disc, was applied to mimic the approaching of a predator in the natural environment. Wild-type larva exhibited a fast C-shape escape response to an approaching looming stimulus (Figure 5I), but this visual behavior was largely impaired in the *VIT* morphant (Figure 5J and 5K).

Apoptosis plays an important role in embryogenesis and tissue homeostasis [54]. The early steps in eye development involve extensive cell death associated with morphogenesis, and the suppression of apoptosis in cells of the lens lineage by fibroblast growth factors is an important component of lens morphogenesis [55]. We therefore examined the role of *VIT* in apoptosis in developing eyes by staining zebrafish embryos with acridine orange (AO). We detected few apoptotic cells in wild-type control zebrafish. In contrast, significantly increased levels of staining were observed throughout the eyes of zebrafish injected with 4 ng of *VIT*-e3i3-MO (the antisense MO oligonucleotide), suggesting increased levels of apoptosis (Figure 6). In addition, we detected increased levels of apoptosis in other tissues including brain and heart (Figure 6, Supplementary information, Figure S8).

All these analyses collectively indicate that the *VIT* gene is necessary for normal physiological function of zebrafish retina, and the evolutionary changes in *VIT* might play a vital role in the evolution of vision in the domestic chicken.

Discussion

By an extensive analysis of the genome sequences of Red Junglefowl and village chickens, we found that a series of vision-related genes have undergone positive selection rather than relaxation of purifying selection in domestic chickens. In particular, *VIT* likely has a function in vision and the evolution of *VIT* might play a role in the evolution of vision in domestic chicken. A caveat of our approach is that the individuals studied possibly do not represent the entirety of genetic variation seen among chickens.

Functional enrichment analysis showed that a group of genes identified by several approaches based on the genomic and transcriptomic data were involved in the vision-related categories. We compared our result with a previous report by Rubin *et al.* [1]. Only limited number of genes overlapped (Supplementary information, Figure S9), among which were two important domestication-related genes, *TSHR* and *TBC1D1*. The limited overlap between our report and study by Rubin *et al.* [1]

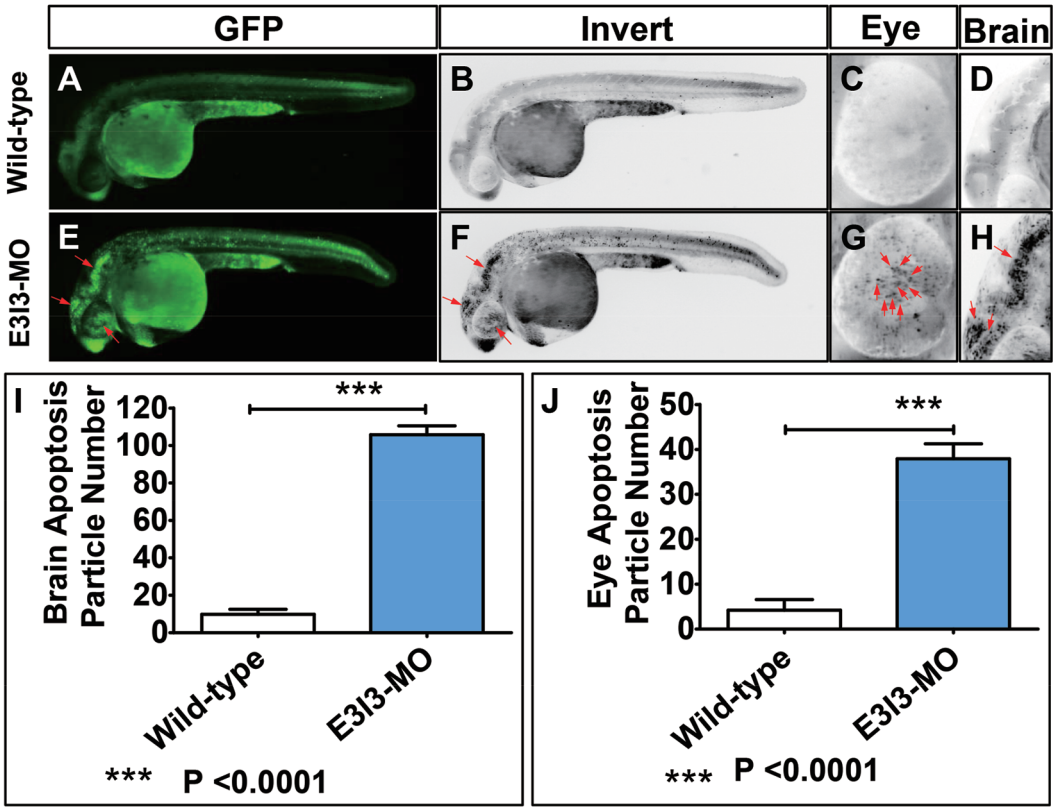

Figure 6 Morpholino knockdown of *VIT* induces potent apoptosis in the eye and brain. Wild-type control embryos and embryos injected with *VIT*-e3i3-MO (E3I3-MO) were stained with acridine orange (AO) at 32 hpf. Apoptotic cells are visible as bright green spots or black spots, and less bright homogenous green or black staining, an unspecific background staining. **(A-D)** Uninjected wild-type control zebrafish exhibited few or no apoptotic cells in whole organism. In contrast, significantly increased staining was observed throughout the brain and eye in zebrafish injected with 4 ng *VIT*-e3i3-MO **(E-H**, red arrows). Lateral view, anterior, left **(A-H)**. **(I)** Quantification of apoptosis particle number in brain shows a 10-fold increase in *VIT* morphants (n = 10) at 32 hpf. **(J)** Quantification of apoptosis particle number in eye shows a 9-fold increase in *VIT* morphants (n = 10) at 32 hpf.

might be due to differences in sequencing and statistical approaches or the use of different chicken breeds. The complicated history of domestic chicken could also contribute to the observed differences [56]. However, functional enrichment analyses of PSGs reported by Rubin and colleagues showed that many of the genes identified in all domestic lines (AD), commercial broiler lines (CB) as well as in layer lines were functionally involved in vision-related categories (Supplementary information, Table S14-S16), which is synonymous with our results. Since the precise nature of the variations that were selected in our study remain unclear, additional functional, biotechnological and physiological experiments will be needed to identify the mechanisms that explain the attenuated vision in domestic chickens.

Using the parsimony principle, the comparatively weaker eyesight in domestic chickens has been explained as a consequence of relaxation of the functional constraints, as domestic chickens are far less dependent on vision for their behaviors like foraging, avoiding predators and mate choice. They live in a predictable farm environment compared to the Red Junglefowl, which does not require acute vision for survival. However, our present study identified many candidate genes involved in the development of vision with signatures of positive selection, including lower nucleotide diversity and long range of haplotype homozygosity, rather than signatures of relaxation of purifying selection. Moreover, the PSGs show significant changes in their expression in the retina between village chickens and Red Junglefowl. Weakened visual ability in domestic chickens as a by-product of artificial selection on other traits, such as large body size, could be another possibility. Larger body size, for instance, could induce larger eyes that may lose optical

sensitivity [3]. Nevertheless, it is implausible that the large number of genes involved in vision with signatures of positive selection identified in our study (Table 1) could be due to hitchhiking with other genes involved in other selected traits, such as body size. First, vision-related genes are distributed on multiple chromosomes, and thus each gene would have to hitchhike. Second, the levels of population differentiation and XP-EHH values within each of the vision-related genes were higher than those for the adjacent regions/genes, showing that hitchhiking could not generate the signatures of selection seen in these vision-related genes (Figure 2).

It is evident that hitchhiking, relaxation of selection or demographic history cannot offer a concrete explanation to our findings. However, nearly 150 years ago, Darwin mentioned a kind of selection that may be unconscious [57]. Given the results of this study, we propose that during domestication, this unconscious selection may have driven the weakening of vision among domestic chickens. Birds gather visual information through a scanning behavior (also known as vigilance) to make decisions relevant for survival (e.g., detecting predators, making mating choices and finding food) [58]. Presumably, the progenitors of domestic chickens that harbored weaker vision may also have possessed a reduced fear response hence vigilance, allowing them to be more easily caught, reared, and domestic by humans. Chickens with higher constant vigilance would not be easily kept in a cage, particularly in the evening, and thus might not have been selected for domestication. In addition, growth and egg production improves with blindness in chickens. Blind chickens tend to thrive better under more crowded conditions than their sighted counterparts [59]. It is therefore plausible to reason that selection on behavior — which is well documented for many domestic species [17] — unknowingly promoted the selection for chickens with weakened vision.

Dogs also harbor weaker visual acuity compared to their wild ancestors, however, in contrast to chickens, there was no evidence for positive selection in vision-related genes in previous studies [14-16]. Vision is important in birds for survival [58], but other sensory abilities including hearing and smell, might play more important roles in mammals. In dogs, many hypotheses have been proposed to explain the tameness necessary for successful domestication [17]. In chickens, besides behavioral evolution, the evolution of vision might have also been important for successful domestication. Clearly, more targeted studies should clarify this hypothesis, but at the moment this explanation offers a compelling model that may shift some of our perspectives on the genetic history of human-driven domestication of key animals, and raise the appreciation of unconscious selection in the characterization of the evolution of domestic animals [60].

Materials and Methods

This study was approved by the Ethics and Experimental Animal Committee of Kunming Institute of Zoology, Chinese Academy of Science, China.

Genomic and RNA-seq data collection

Genome sequences of domestic chickens from the area of origin might be more suitable for revealing the phenotypic changes after early domestication from the Red Junglefowls (RJF), than those from commercial layer and broiler chickens bred during the 20th century in Europe. To identify potential underlying gene/variants responsible for phenotypic changes in domestic chickens, we used genome re-sequencing data with high-depth from 5 RJFs and 8 village chicken (VCs) bred as a food source in the villages of Yunnan Province, Southwest China, an area believed to be one of the origins for domestic chickens [8] (Supplementary information, Table S1). We also obtained RNA-seq data for the retina and four regions of the brain (cerebral cortex, corpus striatum, optic lobe, and cerebellar vermis) from RJF and VC. RNA-seq libraries with insert size around 300 bp were prepared using the Illumina standard RNA-seq library preparation pipeline and sequenced on the Illumina Hiseq 2000 platform (Supplementary information, Table S2). In total, transcriptomes of three retinas, two cerebral cortex, two cerebellar vermis, one corpus striatum and two optic lobes for VCs and two retinas, one cerebral cortex, one cerebellar vermis, one corpus striatum and one optic lobe for RJFs were used to perform comparative analysis. In addition, another ten transcriptomes were re-sequenced to verify the results, including six transcriptomes of three retinas from three RJF, and four transcriptomes of two retinas from two VCs with two experimental repeats per sample on the Hiseq 4000 platform (Supplementary information, Table S2). Sequencing data from this study have been submitted to the NCBI Sequence Read Archive (SRA; http://www.ncbi.nlm.nih.gov/sra) under accession number SRP040477.

Genomic sequence alignment and genotyping

Sequence reads were filtered by removing adaptors and low-quality bases using cutadaptor and Btrim [61] (http://graphics.med.yale.edu/trim/). Only qualified paired-end reads were aligned onto the chicken reference genome (Galgal4) using BWA-MEM with default settings, except "-t 8 -M" options (https://github.com/lh3/bwa). A series of post-processes were then carried out with the alignment bam format file, including sorting, duplicate marking, local realignment and base quality recalibration. All of them were carried out using the relevant tools from the Picards 1.56 (http://picard.sourceforge.net) and Genome Analysis Toolkit 2.6 [62] (GATK). SNPs and indels were called and filtered using UnifiedGenotyper and VariantFiltration command in GATK. Loci with more than 2 alleles were removed. All SNPs were assigned to specific genomic regions and genes using ANNOVAR [63] based on the Ensembl chicken annotations.

A total of 17 115 375 SNPs were identified, around half (51.6%) of which were mapped to intergenic regions in the genome (Sup-

plementary information, Table S3). Among the SNPs that locate to protein-coding regions, 70 990 were non-synonymous and 174 748 were synonymous, with 445 genes (including 446 transcripts) having SNPs that cause the gain or loss of a stop codon (Supplementary information, Table S4).

Genome-wide selective sweep scans

To identify genomic regions harboring footprints of positive selection in native chickens, we employed multiple tests to investigate selection in both populations and in a single population. Here, we used the F_{ST}, *Pi*, XP-EHH and XP-CLR statistical methods. F_{ST} values for each SNP were calculated between RJF and VC as previously described [10]. Nucleotide diversities ($\Delta\pi$ or ΔPi) = $\pi_{RJF} - \pi_{VC}$ were calculated using a sliding window analysis with a window size of 50 kb and a step size of 25 kb. XP-EHH value for each variant was calculated according to [11]. XP-CLR test [12] was performed with scripts available at http://genetics.med.harvard.edu/reich/Reich_Lab/Software.html using the following parameters: sliding window size 0.1 cM, grid size 10 k, maximum number of SNPs within a window 300, correlation value for 2 SNPs weighted with a cutoff of 0.99. Here, VC was taken to be the object population, and RJF was chosen as the reference population. Haplotypes for each chromosome were deduced by shapeit.v2.r727 [64] (http://www.shapeit.fr/). General genetic map for chicken used here was 2.8 cM/Mb for chr1-9 and 6.4 cM/Mb for chr10-28 and chr32 [65].

SNP validation in larger population

We choose 67 SNPs that were mapped to the *TSHR*, *ATP13A4*, *RPGRIP1L*, *COL18A1*, *VIT*, *OPA1*, *IGF2BP3* and *MAP3K5* genes (see Supplementary information, Table S5) to validate in larger population, including ~25 RJFs and ~20 VCs by Sanger sequencing. Primer pairs used for these genes are listed in Supplementary information, Table S6.

Demographic history and coalescent simulations

Demographic histories for RJF and VC were inferred using MSMC [66] based on haplotypes from multiple individuals in each population. We performed our analysis using 2 individuals (4 haplotypes), 3 individuals (6 haplotypes), 4 individuals (8 haplotypes) and 5 individuals (10 haplotypes) for each group (VC and RJF) independently. To assess the significance of the selective sweep signals identified by the above-mentioned methods, we stimulated two groups of genome sequences (one for VC and one for RJF) under a neutral evolutionary model taking into account the inferred demographic history. Coalescent simulations were performed using the ms program [67]. In total, 26 sequences of 50 kb were simulated 1 000 times and applied to the F_{ST} and *Pi* test. In addition, 26 sequences of 1 Mb were simulated 1 000 times and the mean XP-EHH value of the middle 50 kb (475-525 kb) in each simulated sequence was calculated as simulated data. Population sizes for the common ancestors (> 8 kya and ~2 kya) of RJF and VC were obtained from our MSMC analysis. Since MSMC has a low power to estimate population size at relatively recent times, the effective population sizes for present day RJF and VC populations were taken from elsewhere [68] (1.6×10^5 and 4×10^5, respectively). Generation time (g) and mutation rate per year (u) for chicken used here is 1 year and 1.91×10^{-9}, respectively [69].

Scripts used for simulation were as follows:

For F_{ST} and *Pi:*

ms 26 1000 -T -I 2 10 16 -t 191 -en 0.003 1 0.16 -en 0.003 2 0.22 -en 0.001 1 0.8 -eg 0.001 1 0 -en 0.001 2 0.32 -eg 0.001 2 0 -ej 0.004 1 2 | tail -n +4 | grep -v // >fst-pi-treefile

seq-gen -mHKY -l 50000 -s .017 <fst-pi-treefile> fst-pi-seqfile.ms

For XP-EHH:

ms 26 1000 -I 2 10 16 -t 3820 -en 0.003 1 0.16 -en 0.003 2 0.22 -en 0.001 1 0.8 -eg 0.001 1 0 -en 0.001 2 0.32 -eg 0.001 2 0 -ej 0.004 1 2 -p 6 >XP-EHH.ms

Test for the effect of relaxation of constraints and hitchhiking

Relaxation of purifying selection should increase pN/pS (the ratio of the number of non-synonymous substitutions per non-synonymous site (N) to the number of synonymous substitutions per synonymous site (S)) as selection against non-synonymous substitutions is lowered [41, 42]. Here, we retrieved SNPs in vision-related genes identified under potential positive selection by the four methods, according to functional category enrichment, and calculated the ratio of the number of pN SNPs to the number of synonymous SNPs (N/S) in the VC and RJF populations. To exclude the possibility of hitchhiking, we compared the F_{ST}, *Pi* and XP-EHH values for the visual-related candidate genes with their related upstream/downstream sequences of the same length as the gene, sequences at distance of 50 kb and in adjacent genes.

Comparison of gene expression

The RNA-seq data were trimmed to filter out adaptor sequences and low-quality bases using cutadaptor and Btrim (http://graphics.med.yale.edu/trim/) and were mapped onto the chicken reference using Tophat [43, 70]. Cufflinks and cuffcompare [43] were then used to assemble transcripts and compare the assembled transcripts with the annotated reference transcripts, generating a newmerged GTF annotation file. New transcripts assembled here were defined as: having at least 2 exons and length ≥ 200 bp with class code j, c, o, e, and new loci with all class codes being u, or i, or x. Cufflinks was run using the GTF file with parameter "-G" to retrieve expression profile for each gene. Cuffdiff [43] was used to detect the significance of the gene expression differences from four brain regions (cerebral cortex, corpus striatum, optic lobe, and cerebellar vermis) and retina between the RJF and VC. *P*-value was corrected by FDR (default by cuffdiff program).

To assess whether the expression changes in retina, cerebral cortex, corpus striatum, optic lobe, and cerebellar vermis between RJF and VC may have been driven by positive selection at local regulatory sites during domestication, a series of statistic tests were performed. The expression level (FPKM) for each gene in each tissue was retrieved and transformed according to $\log_2$(FPKM + 1) [68]. The difference of expression level for each gene between VC and RJF was calculated using $\log_2((FPKM + 1)_{VC}/(FPKM + 1)_{RJF})$. We then compared the expression levels of PSGs identified by F_{ST}, *Pi*, XP-EHH and XP-CLR with those of other genes (all genes in whole genome excluding PSGs) by Mann-Whitney *U* test and Kolmogorov-Smirnov test in each tissue. *P*-values were corrected by FDR. Since the two different batches of data employed different sequencing platforms and different runs, we performed the comparative analysis on data generated on the Hiseq 2000 and the Hiseq 4000 platforms independently, and also analyzed the combined

data generated on both platforms.

Selective sweep region annotation and gene functional enrichment analysis

Candidates' selective sweeps detected by the above-mentioned methods were annotated using the Variant Effect Predictor available at http://asia.ensembl.org/info/docs/tools/index.html. Functional enrichments of the protein-coding genes including GO categories, KEGG pathway and HPO were analyzed using g: Profiler [71].

VIT expression data in mouse

Expression data for *VIT* in different tissues of the mouse was retrieved from Biogps (http://biogps.org/). Expression profiling by array in retinal pigment epithelium (RPE) of mouse exposed to 10 000 lux of cool white fluorescent light for 18 h was from a previous study [72] (GSE37773). The expression data from retina after *Hmx1* loss and in wild-type mice were from another study [73] (GSE47002). Expression data from photoreceptor cells of $Nrl^{-/-}$ mice and $Crx::Nr2e3/Nrl^{-/-}$ mice were also from a previous study [46] (GSE5338).

RNA extraction and real-time quantitative PCR assay

Total RNA was isolated from chicken retina tissues using TRNzol-A+ (Tiangen Biotech, Beijing, China) and purified using RNeasy Micro kit (Qiagen, Germany). Concentration and integrity of the RNA was measured using electrophoresis and NanoDrop spectrophotometer 2000. Total RNA (2 μg) was used to synthesize single-strand cDNA using the PrimeScript RT-PCR Kit (TaKaRa, Japan) in a final volume of 25 μL reaction mixture according to the manufacturer's instructions. The relative mRNA expression levels of *RPGR* (retinitis pigmentosa GTPase regulator), *GUCAIA* (guanylate cyclase activator 1A), *TRPM1* (transient receptor potential cation channel, subfamily M, member 1), *PDE6B* (phosphodiesterase 6B), *NR2E3* (nuclear receptor subfamily 2, group E, member 3), *VIT* (vitrin) and *RHO* (rhodopsin) genes were measured using real-time quantitative PCR (qPCR) and the relative standard curve method, with normalization to the house-keeping gene *GAPDH*. qPCR was performed on the platform of the iQ2 system (BioRad Laboratories, Hercules, CA, USA) with SYBR Premix Ex Taq II kit (TaKaRa, DRR081A). Student's *t*-test was used to analyze the differences and measure the statistical significance. Primer pairs used for these genes are listed in Supplementary information, Table S7.

Zebrafish care and maintenance

Adult wild-type AB strain zebrafish were maintained at 28.5 °C on a 14 h light/10 h dark cycle [74]. Five to six pairs of zebrafish were set up for each natural mating each time. On average, 200-300 embryos were generated. Embryos were maintained at 28.5 °C in fish water (0.2% Instant Ocean Salt in deionized water). The embryos were washed and staged according to published guidelines [75]. The zebrafish facility at Shanghai Research Center for Model Organisms is accredited by the Association for Assessment and Accreditation of Laboratory Animal Care (AAALAC) International.

Zebrafish microinjections

Gene Tools, LLC (http://www.gene-tools.com/) designed the MO oligonucleotide. Antisense MO (GeneTools) was microinjected into fertilized one-cell stage embryos according to standard protocols [76]. The sequence of the exon 3-intron 3 splice *VIT* MO (*VIT*-e3i3-MO) was 5′-CCTGAATAGTCTACAGTACCTGAGA-3′. For the *VIT* knockdown experiment, 4 ng of *VIT*-e3i3-MO was used per injection. Total RNA was extracted from 80 to 100 embryos per group in Trizol (Invitrogen) according to the manufacturer's instructions. RNA was reverse transcribed using the PrimeScript RT reagent Kit with gDNA Eraser (Takara). Primers spanning *VIT* exon 2 (forward primer: 5′-GTTCGCCTCCATATCCAGCATCTGC-3′) and exon 9 (reverse primer: 5′-TTCCCCTGGACGCTCTGAGACTGTC-3′) were used for RT-PCR analysis for confirmation of the efficacy of the E3I3-MO.

AO staining for apoptosis

Wild-type control embryos and embryos injected with 4 ng *VIT*-e3i3-MO were immersed in 5 μg/ml AO (acridinium chloride hemi-[zinc chloride], Sigma-Aldrich) in fish water for 60 min at 32-hpf and 80-hpf. Next, zebrafish were rinsed thoroughly in fish water three times (5 min/wash) and anaesthetized with 0.016% MS-222 (Tricaine methanesulfonate, Sigma-Aldrich, St. Louis, MO). Zebrafish were then oriented on their lateral side and mounted with methylcellulose in a depression slide for observation by fluorescence microscopy.

In vivo ERG recording

Zebrafish larvae were first paralyzed with α-bungarotoxin (100 μg/ml, Sigma), and then embedded in 1% low melting-point agarose (Sigma) with one eye upward in a custom-made chamber as described previously [77]. The cornea and lens of the upward eye were removed to expose retinal surface by using a glass micropipette with a tip opening of 1 μm. After dissection, the larvae were transferred to a recording setup, and perfused with extracellular solution, which consists of (in mM) 134 NaCl, 2.9 KCl, 4 $CaCl_2$, 10 HEPES and 10 glucose (290 mOsmol/l, pH 7.8). ERG responses were recorded with an EPC-10 amplifier (Heka, Germany) through inserting the pipette of ~3-μm tip opening into the interface of photoreceptors and bipolar cells. The ERG signals were amplified at 1 000 total gain and low-pass filtered at 100 Hz. Whole-field light stimuli were given by a white LED controlled by the Master 8 stimulator (A.M.P.I., Israel).

Visual escape behavioral test

Larval behavior was monitored by an infrared-sensitive high-speed camera at the acquisition rate of 250 Hz (Redlake Motionscope M3, US). In one experiment, the behaviors of 12 larvae were simultaneously recorded. Each larva was put in an individual 3.5-cm Petri dish under the light background for 30 min to adapt. During each test, 10 trials were carried out for calculating the probability of escape behavior with a 5-min interval. A successful escape was scored when a C-shape movement finished within 20 ms after movement onset [78]. Visual stimuli were generated by a self-written Matlab program and delivered through a mini-projector. The dark shadow would gradually cover the fish's body when an expanding black disc was projected on the Petri dish at the expanding speed of ~5.4 cm/s.

Image acquisition

Embryos and larvae were analyzed with Nikon SMZ 1500 fluorescence microscope and subsequently photographed with digital cameras. A subset of images was adjusted for levels,

brightness, contrast, hue and saturation with Adobe Photoshop 7.0 software (Adobe, San Jose, CA, USA) to optimally visualize the expression patterns. Quantitative image analyses processed using image-based morphometric analysis (NIS-Elements D3.1, Japan) and ImageJ software (National Institutes of Health, Bethesda, MD, USA; http://rsbweb.nih.gov/ij/). Inverted fluorescent images were used for processing. Positive signals were defined by particle number using ImageJ. In total, 10 animals for each treatment were analyzed and the total signals per animal were averaged. All data were presented as mean ± SEM. Statistical analysis and graphical representation of the data were performed using GraphPad Prism 5.0 (GraphPad Software, San Diego, CA, USA). Statistical significance was performed using a Student's *t*-test as appropriate. Statistical significance is indicated by *, where $P < 0.05$, and ***, where $P < 0.0001$.

Acknowledgments

We thank Andrew Willden and Newton O Otecko for language editing of the manuscript. This work was supported by the Breakthrough Project of Strategic Priority Program of the Chinese Academy of Sciences (XDB13000000), the National Natural Science Foundation of China (91331104), the 973 program (2013CB835200, 2013CB835204), and Bureau of Science and Technology of Yunnan Province, and the Youth Innovation Promotion Association, Chinese Academy of Sciences.

Author Contributions

YPZ and DDW led the project and designed the study. MSW, RWZ, LYS and JLD performed experiments. MSW, DDW, LYS, YL, MSP, RWZ, JLD, HQL and LZ performed the analyses. MSW, HQL and LZ sampled chickens and tissues. MSW, DDW, DMI and YGY drafted the manuscript. All authors read and improved the manuscript.

Competing Financial Interests

The authors declare no competing financial interests.

References

1 Rubin CJ, Zody MC, Eriksson J, *et al.* Whole-genome resequencing reveals loci under selection during chicken domestication. *Nature* 2010; **464**:587-591.
2 Yokoyama S. Molecular evolution of color vision in vertebrates. *Gene* 2002; **300**:69-78.
3 Roth LS, Lind O. The impact of domestication on the chicken optical apparatus. *PLoS One* 2013; **8**:e65509.
4 Lisney TJ, Rubene D, Rozsa J, Lovlie H, Hastad O, Odeen A. Behavioural assessment of flicker fusion frequency in chicken *Gallus gallus* domesticus. *Vision Res* 2011; **51**:1324-1332.
5 Lisney TJ, Ekesten B, Tauson R, Hastad O, Odeen A. Using electroretinograms to assess flicker fusion frequency in domestic hens *Gallus gallus* domesticus. *Vision Res* 2012; **62**:125-133.
6 Peichl L. Topography of ganglion cells in the dog and wolf retina. *J Comp Neurol* 1992; **324**:603-620.
7 Evans KE, McGreevy PD. The distribution of ganglion cells in the equine retina and its relationship to skull morphology. *Anat Histol Embryol* 2007; **36**:151-156.
8 Miao YW, Peng MS, Wu GS, *et al.* Chicken domestication: an updated perspective based on mitochondrial genomes. *Heredity* 2013; **110**:277-282.
9 Sabeti PC, Schaffner SF, Fry B, *et al.* Positive natural selection in the human lineage. *Science* 2006; **312**:1614-1620.
10 Akey JM, Zhang G, Zhang K, Jin L, Shriver MD. Interrogating a high-density SNP map for signatures of natural selection. *Genome Res* 2002; **12**:1805-1814.
11 Sabeti PC, Varilly P, Fry B, *et al.* Genome-wide detection and characterization of positive selection in human populations. *Nature* 2007; **449**:913-918.
12 Chen H, Patterson N, Reich D. Population differentiation as a test for selective sweeps. *Genome Res* 2010; **20**:393-402.
13 Akey JM. Constructing genomic maps of positive selection in humans: where do we go from here? *Genome Res* 2009; **19**:711-722.
14 Axelsson E, Ratnakumar A, Arendt ML, *et al.* The genomic signature of dog domestication reveals adaptation to a starch-rich diet. *Nature* 2013; **495**:360-364.
15 Li Y, Vonholdt BM, Reynolds A, *et al.* Artificial selection on brain-expressed genes during the domestication of dog. *Mol Biol Evol* 2013; **30**:1867-1876.
16 Wang GD, Zhai W, Yang HC, *et al.* The genomics of selection in dogs and the parallel evolution between dogs and humans. *Nat Commun* 2013; **4**:1860.
17 Li Y, Wang GD, Wang MS, Irwin DM, Wu DD, Zhang YP. Domestication of the dog from the wolf was promoted by enhanced excitatory synaptic plasticity: a hypothesis. *Genome Biol Evol* 2014; **6**:3115-3121.
18 Carneiro M, Rubin CJ, Di Palma F, *et al.* Rabbit genome analysis reveals a polygenic basis for phenotypic change during domestication. *Science* 2014; **345**:1074-1079.
19 Vallipuram J, Grenville J, Crawford DA. The E646D-ATP13A4 mutation associated with autism reveals a defect in calcium regulation. *Cell Mol Neurobiol* 2010; **30**:233-246.
20 Lesca G, Rudolf G, Labalme A, *et al.* Epileptic encephalopathies of the Landau-Kleffner and continuous spike and waves during slow-wave sleep types: genomic dissection makes the link with autism. *Epilepsia* 2012; **53**:1526-1538.
21 Worthey EA, Raca G, Laffin JJ, *et al.* Whole-exome sequencing supports genetic heterogeneity in childhood apraxia of speech. *J Neurodev Disord* 2013; **5**:29.
22 Kwasnicka-Crawford DA, Carson AR, Roberts W, *et al.* Characterization of a novel cation transporter ATPase gene (ATP13A4) interrupted by 3q25-q29 inversion in an individual with language delay. *Genomics* 2005; **86**:182-194.
23 Lu B, Zhang Q, Wang H, Wang Y, Nakayama M, Ren D. Extracellular calcium controls background current and neuronal excitability via an UNC79-UNC80-NALCN cation channel complex. *Neuron* 2010; **68**:488-499.
24 Stray-Pedersen A, Cobben JM, Prescott TE, *et al.* Biallelic mutations in UNC80 cause persistent hypotonia, encephalopathy, growth retardation, and severe intellectual disability. *Am J Hum Genet* 2016; **98**:202-209.
25 Fan WL, Ng CS, Chen CF, *et al.* Genome-wide patterns of genetic variation in two domestic chickens. *Genome Biol Evol* 2013; **5**:1376-1392.
26 Hartmann EM, Bea S, Navarro A, *et al.* Increased tumor cell proliferation in mantle cell lymphoma is associated with el-

evated insulin-like growth factor 2 mRNA-binding protein 3 expression. *Mod Pathol* 2012; **25**:1227-1235.
27 Jones JI, Clemmons DR. Insulin-like growth factors and their binding proteins: biological actions. *Endocr Rev* 1995; **16**:3-34.
28 Suvasini R, Shruti B, Thota B, *et al.* Insulin growth factor-2 binding protein 3 (IGF2BP3) is a glioblastoma-specific marker that activates phosphatidylinositol 3-kinase/mitogen-activated protein kinase (PI3K/MAPK) pathways by modulating IGF-2. *J Biol Chem* 2011; **286**:25882-25890.
29 Lin S, Li H, Mu H, *et al.* Let-7b regulates the expression of the growth hormone receptor gene in deletion-type dwarf chickens. *BMC Genomics* 2012; **13**:306.
30 Lechner J, Porter LF, Rice A, *et al.* Enrichment of pathogenic alleles in the brittle cornea gene, *ZNF469*, in keratoconus. *Hum Mol Genet* 2014; **23**:5527-5535.
31 Rohrbach M, Spencer HL, Porter LF, *et al.* ZNF469 frequently mutated in the brittle cornea syndrome (BCS) is a single exon gene possibly regulating the expression of several extracellular matrix components. *Mol Genet Metab* 2013; **109**:289-295.
32 Azadi S, Molday LL, Molday RS. RD3, the protein associated with Leber congenital amaurosis type 12, is required for guanylate cyclase trafficking in photoreceptor cells. *Proc Natl Acad Sci USA* 2010; **107**:21158-21163.
33 Duh EJ, Yao YG, Dagli M, Goldberg MF. Persistence of fetal vasculature in a patient with Knobloch syndrome: Potential role for endostatin in fetal vascular remodeling of the eye. *Ophthalmology* 2004; **111**:1885-1888.
34 Sertie AL, Sossi V, Camargo AA, Zatz M, Brahe C, Passos-Bueno MR. Collagen XVIII, containing an endogenous inhibitor of angiogenesis and tumor growth, plays a critical role in the maintenance of retinal structure and in neural tube closure (Knobloch syndrome). *Hum Mol Genet* 2000; **9**:2051-2058.
35 Fukai N, Eklund L, Marneros AG, *et al.* Lack of collagen XVIII/endostatin results in eye abnormalities. *EMBO J* 2002; **21**:1535-1544.
36 Ylikarppa R, Eklund L, Sormunen R, *et al*. Lack of type XVIII collagen results in anterior ocular defects. *FASEB J* 2003; **17**:2257-2259.
37 Marneros AG, Olsen BR. Age-dependent iris abnormalities in collagen XVIII/endostatin deficient mice with similarities to human pigment dispersion syndrome. *Invest Ophthalmol Vis Sci* 2003; **44**:2367-2372.
38 Li Q, Olsen BR. Increased angiogenic response in aortic explants of collagen XVIII/endostatin-null mice. *Am J Pathol* 2004; **165**:415-424.
39 Ferre M, Bonneau D, Milea D, *et al.* Molecular screening of 980 cases of suspected hereditary optic neuropathy with a report on 77 novel OPA1 mutations. *Hum Mutat* 2009; **30**:E692-E705.
40 Amati-Bonneau P, Milea D, Bonneau D, *et al.* OPA1-associated disorders: phenotypes and pathophysiology. *Int J Biochem Cell Biol* 2009; **41**:1855-1865.
41 Bjornerfeldt S, Webster MT, Vila C. Relaxation of selective constraint on dog mitochondrial DNA following domestication. *Genome Res* 2006; **16**:990-994.
42 Wang Z, Yonezawa T, Liu B, *et al.* Domestication relaxed selective constraints on the yak mitochondrial genome. *Mol Biol Evol* 2011; **28**:1553-1556.
43 Trapnell C, Roberts A, Goff L, *et al.* Differential gene and transcript expression analysis of RNA-seq experiments with TopHat and Cufflinks. *Nat Protoc* 2012; **7**:562-578.
44 Wilson JH, Wensel TG. The nature of dominant mutations of rhodopsin and implications for gene therapy. *Mol Neurobiol* 2003; **28**:149-158.
45 Cheng H, Khanna H, Oh EC, Hicks D, Mitton KP, Swaroop A. Photoreceptor-specific nuclear receptor NR2E3 functions as a transcriptional activator in rod photoreceptors. *Hum Mol Genet* 2004; **13**:1563-1575.
46 Cheng H, Aleman TS, Cideciyan AV, Khanna R, Jacobson SG, Swaroop A. *In vivo* function of the orphan nuclear receptor NR2E3 in establishing photoreceptor identity during mammalian retinal development. *Hum Mol Genet* 2006; **15**:2588-2602.
47 Haider NB, Naggert JK, Nishina PM. Excess cone cell proliferation due to lack of a functional NR2E3 causes retinal dysplasia and degeneration in *rd7*/*rd7* mice. *Hum Mol Genet* 2001; **10**:1619-1626.
48 Kono M, Goletz PW, Crouch RK. 11-cis- and all-trans-retinols can activate rod opsin: rational design of the visual cycle. *Biochemistry* 2008; **47**:7567-7571.
49 Kong YF, Karplus M. The signaling pathway of rhodopsin. *Structure* 2007; **15**:611-623.
50 Beltran WA, Cideciyan AV, Lewin AS, *et al.* Gene therapy rescues photoreceptor blindness in dogs and paves the way for treating human X-linked retinitis pigmentosa. *Proc Natl Acad Sci USA* 2012; **109**:2132-2137.
51 Morgans CW, Zhang J, Jeffrey BG, *et al.* TRPM1 is required for the depolarizing light response in retinal ON-bipolar cells. *Proc Natl Acad Sci USA* 2009; **106**:19174-19178.
52 Wright RN, Hong DH, Perkins B. Misexpression of the constitutive Rpgr(ex1-19) variant leads to severe photoreceptor degeneration. *Invest Ophthalmol Visual Sci* 2011; **52**:5189-5201.
53 Wong KY, Gray J, Hayward CJ, Adolph AR, Dowling JE. Glutamatergic mechanisms in the outer retina of larval zebrafish: analysis of electroretinogram b- and d-waves using a novel preparation. *Zebrafish* 2004; **1**:121-131.
54 Abud HE. Shaping developing tissues by apoptosis. *Cell Death Differ* 2004; **11**:797-799.
55 Lang RA. Apoptosis in mammalian eye development: lens morphogenesis, vascular regression and immune privilege. *Cell Death Differ* 1997; **4**:12-20.
56 Liu YP, Wu GS, Yao YG, *et al*. Multiple maternal origins of chickens: out of the Asian jungles. *Mol Phylogenet Evol* 2006; **38**:12-19.
57 Darwin C. The Variation of Animals and Plants Under Domestication 1868.
58 Fernandez-Juricic E. Sensory basis of vigilance behavior in birds: synthesis and future prospects. *Behav Process* 2012; **89**:143-152.
59 Sandøe P, Hocking PM, Förkman B, Haldane K, Kristensen HH, Palmer C. The blind hens' challenge: does it undermine the view that only welfare matters in our dealings with animals? *Environ Value* 2014; **23**:727-742.
60 Larson G, Fuller DQ. The evolution of animal domestication.

Annu Rev Ecol Evol Syst 2014; **45**:115-136.
61 Kong Y. Btrim: a fast, lightweight adapter and quality trimming program for next-generation sequencing technologies. *Genomics* 2011; **98**:152-153.
62 McKenna A, Hanna M, Banks E, *et al.* The Genome Analysis Toolkit: a MapReduce framework for analyzing next-generation DNA sequencing data. *Genome Res* 2010; **20**:1297-1303.
63 Wang K, Li M, Hakonarson H. ANNOVAR: functional annotation of genetic variants from high-throughput sequencing data. *Nucleic Acids Res* 2010; **38**:e164.
64 Delaneau O, Zagury JF, Marchini J. Improved whole-chromosome phasing for disease and population genetic studies. *Nat Methods* 2013; **10**:5-6.
65 Axelsson E, Webster MT, Smith NG, Burt DW, Ellegren H. Comparison of the chicken and turkey genomes reveals a higher rate of nucleotide divergence on microchromosomes than macrochromosomes. *Genome Res* 2005; **15**:120-125.
66 Schiffels S, Durbin R. Inferring human population size and separation history from multiple genome sequences. *Nat Genet* 2014; **46**:919-925.
67 Hudson RR. Generating samples under a Wright-Fisher neutral model of genetic variation. *Bioinformatics* 2002; **18**:337-338.
68 Lee S, Seo CH, Lim B, *et al.* Accurate quantification of transcriptome from RNA-Seq data by effective length normalization. *Nucleic Acids Res* 2011; **39**:e9.
69 Nam K, Mugal C, Nabholz B, *et al.* Molecular evolution of genes in avian genomes. *Genome Biol* 2010; **11**:R68.
70 Trapnell C, Pachter L, Salzberg SL. TopHat: discovering splice junctions with RNA-Seq. *Bioinformatics* 2009; **25**:1105-1111.
71 Reimand J, Arak T, Vilo J. g:Profiler--a web server for functional interpretation of gene lists (2011 update). *Nucleic Acids Res* 2011; **39**:W307-W315.
72 Hadziahmetovic M, Kumar U, Song Y, *et al.* Microarray analysis of murine retinal light damage reveals changes in iron regulatory, complement, and antioxidant genes in the neurosensory retina and isolated RPE. *Invest Ophthalmol Visual Sci* 2012; **53**:5231-5241.
73 Boulling A, Wicht L, Schorderet DF. Identification of HMX1 target genes: A predictive promoter model approach. *Mol Vis* 2013; **19**:1779-1794.
74 Westerfield M. The zebrafish book: A guide for the laboratory use of zebrafish. Eugene. The University of Oregon Press 1993.
75 Kimmel CB, Ballard WW, Kimmel SR, Ullmann B, Schilling TF. Stages of embryonic development of the zebrafish. *Dev Dyn* 1995; **203**:253-310.
76 Nasevicius A, Ekker SC. Effective targeted gene 'knockdown' in zebrafish. *Nat Genet* 2000; **26**:216-220.
77 Zhang RW, Wei HP, Xia YM, Du JL. Development of light response and GABAergic excitation-to-inhibition switch in zebrafish retinal ganglion cells. *J Physiol* 2010; **588**:2557-2569.
78 Mu Y, Li XQ, Zhang B, Du JL. Visual input modulates audiomotor function via hypothalamic dopaminergic neurons through a cooperative mechanism. *Neuron* 2012; **75**:688-699.

(**Supplementary information** is linked to the online version of the paper on the *Cell Research* website.)